In Situ Observation of Thermal Relaxation of Interstitial-Vacancy Pair Defects in a Graphite Gap

Koki Urita,[1] Kazu Suenaga,[1,*] Toshiki Sugai,[2] Hisanori Shinohara,[2] and Sumio Iijima[1]

[1]*Research Center for Advanced Carbon Materials, National Institute of Advanced Industrial Science and Technology (AIST), Tsukuba, 305-8565, Japan*

[2]*Department of Chemistry and Institute for Advanced Research, Nagoya University, Nagoya, 464-8602, Japan*

(Received 10 December 2004; published 20 April 2005)

Direct observation of individual defects during formation and annihilation in the interlayer gap of double-wall carbon nanotubes (DWNT) is demonstrated by high-resolution transmission electron microscopy. The interlayer defects that bridge two adjacent graphen layers in DWNT are stable for a macroscopic time at the temperature below 450 K. These defects are assigned to a cluster of one or two interstitial-vacancy pairs (*I*-*V* pairs) and often disappear just after their formation at higher temperatures due to an instantaneous recombination of the interstitial atom with vacancy. Systematic observations performed at the elevated temperatures find a threshold for the defect annihilation at 450–500 K, which, indeed, corresponds to the known temperature for the Wigner energy release.

DOI: 10.1103/PhysRevLett.94.155502 PACS numbers: 61.72.Ji, 61.72.Ff, 61.80.Lj, 81.07.De

The formation and relaxation of lattice defects in crystal govern the physical properties of a solid and therefore have long been under intensive investigations in the field of physics. The kinetics of lattice disordering and thermal relaxation so far has been discussed only from the macroscopic viewpoint, but has never been investigated from an atomic viewpoint where activities of individual defects can be monitored. The defect formation and relaxation behavior of graphite materials under high-energy beam irradiation is of great scientific and technological importance [1,2]. The interlayer defect ''in between'' two adjacent layers is particularly crucial for graphite in practical uses, such as a graphite moderator employed for a nuclear reactor, and has long been believed to appear frequently under energetic beam irradiation [3]. Theoretical studies have suggested a metastable Frenkel-type defect, which consists of an interstitial carbon atom and a vacancy [the interstitial and vacancy (*I*-*V*) pair] in between bilayer graphite [3,4]. Any direct evidence for this type of interlayer defect, which can be stable for a macroscopic time but is likely to annihilate, has not been provided so far.

The temperature dependence of the formation and relaxation behavior of the atomic defects is extremely intriguing. Because a vacancy and an extra atom are believed to recombine and disappear instantaneously when both come closer, a stable *I*-*V* pair defect requires a recombination barrier. As the electron irradiation damage rate (the knock-on frequency) is not very dependent on the temperature, the occurrence of defect formation can be mostly dominated by its energetics. Our previous work demonstrated the stable defects in ''single'' graphen layers at room temperature by means of *in situ* high-resolution transmission electron microscopy (HR-TEM) with atomic sensitivity [5], and, indeed, suggested a high recombination barrier. Further experiments for ''stacking'' graphite extended at various temperatures are definitively required in order to corroborate the annealing effect of defective graphite. The results should provide important implications for the source of the energy stored in irradiated graphite, which has been a well-known problem for more than half a century [6,7].

An ideal test object for the HR-TEM observation of the interlayer defect formation is a double-wall carbon nanotube (DWNT). There are two major reasons for employing the DWNTs: (i) A DWNT consists of a bilayer graphite and is the thinnest specimen for HR-TEM observation of the interlayer defects. [Note that a single-atomic defect would become more and more difficult to be imaged in a thicker specimen such as highly oriented pyrolitic graphite (HOPG).] (ii) Both the top-wall and side-wall defects can easily be imaged at the same time, and a reasonable atomic model for the defect structure can be more convincingly proposed. We should note, however, that the DWNT is representative for the turbostratic graphite but not for the HOPG with the regular *c*-axis stacking. The interlayer orientational relationship is mostly random, and the interlayer distance is slightly larger in DWNTs (0.38 nm) than that for HOPG (0.335 nm) [8]. Also the energetics of defect formations can be affected by the curvature of the graphene layer in DWNT and should therefore be somehow different from that for the flat HOPG.

To visualize the formation of interlayer defects in DWNTs, we have operated a field emission TEM (JEOL-2010F) with the specimen stages at variable temperatures (Gatan 626 DH for cryo-observations and EM 21130 for high-temperature observations). The accelerating voltage has been chosen as 120 kV which is just close to the threshold of the knock-on effect of carbon [9,10]. The DWNTs prepared by a pulsed arc discharge method [11] were dispersed and fixed on microscopy specimen grids. Experimental conditions for visualization of graphite layers have been described in our previous paper [5]. We have chosen the Scherzer defocus value in this experiment; therefore, the zigzag chain contrast (0.21 nm apart) is less

visible compared with the previously reported conditions especially at higher temperatures. The electron dose is estimated as 60 000 electrons per nm^2 for 1 s exposure. We can estimate, by means of semiquantitative image simulation in comparison with the standard deviation of the charge coupled device (CCD) readout noise, that the confidence level for the detection of single vacancy in DWNT is as little as 50%, whereas that for a cluster of two *I*-*V* pairs should be about 80%. One should recall here that a single-atomic defect in DWNT is essentially less visible than the one in SWNT because of a larger total thickness for DWNTs leading to a degraded signal-to-noise ratio.

Figure 1 shows two sequential HR-TEM images of the DWNTs recorded at 573 K. In the first sequential images [Figs. 1(a)–1(d)], several bridges in dark contrast (indicated by red arrows) obviously appear in between two layers. As can be seen more clearly in a few supplemental movie files [12], these interlayer bridges are often appearing and disappearing during the observation. Also in the other sequential images [Figs. 1(e)–1(h)], pairs of dark and bright spots are appearing [Figs. 1(f) and 1(g)] and disappearing just after [Figs. 1(g) and 1(h)] in the middle of the DWNT (see also the second movie file [12]). Both sequential images are attributed to the side and top views of the similar interlayer defects.

There is a tendency that the top-wall defects are more likely to be generated, as Smith and Luzzi suggested [13].

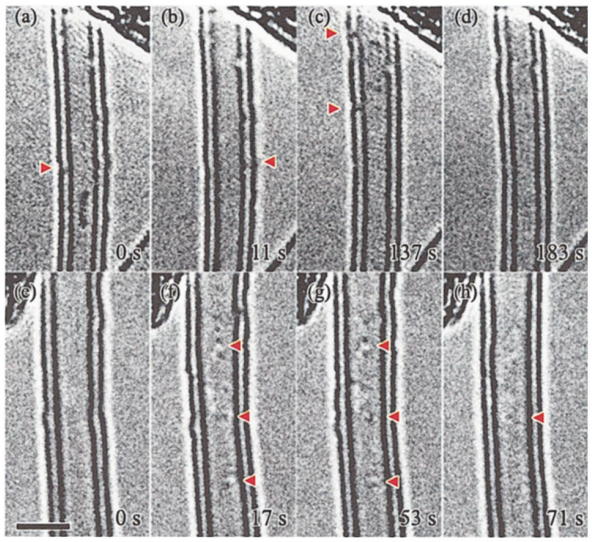

FIG. 1 (color). Sequential HR-TEM images of the interlayer defects which appear and disappear in DWNTs recorded at 573 K. In the side wall (a)–(d), several bridges connecting two graphene layers frequently appear in dark contrast (marked by red arrows) and disappear just after the observation. Also in the top wall (e)–(h), pairs of dark and bright contrast often appear and then vanish (marked by red arrows). See also the movie files available at our Web site (KU01.mov and KU02.mov). Scale bar = 2 nm.

This anisotropy of the defect formation rate between top and side walls seems more prominent at lower temperatures. In the irradiation experiments of DWNTs, the inner nanotube always suffers damage faster than the outer nanotube, and the outer nanotube seems more resistive. This is because the inner nanotube exhibits a larger curvature (a smaller diameter) and more easily suffers knock-on damage. Therefore, we can reasonably assume that the vacancy is more likely to be generated in the inner nanotube.

In order to characterize the atomic structure of these interlayer defects as precisely as possible, the HR-TEM image simulations of the theoretically predicted defect structures have been performed and compared with the experimental images. We have first referred to a model based on the *ab initio* calculation for the *I*-*V* pair in bilayer graphite in the literature [4] and then relaxed the structure to fit within the DWNT gap by using a semiempirical potential. Vacancy has been assumed in the inner layer of DWNT. Figure 2 shows the obtained model structures, involving (a) a single and (b) a couple of *I*-*V* pairs at the interlayer space in the side and top walls. The latter consists of an isolated interstitial pair and a divacancy [14]. The simulated HR-TEM images calculated from these *I*-*V* pairs are also shown in Figs. 2(c) and 2(d). Although the detailed atomic structure of the defect cannot be experimentally derived, the calculated image exhibits an approximate agreement with the observed images [Figs. 1(a)–1(d)]; i.e., the dark contrast bridging the two layers experimentally observed is clearly reproduced. Also, as for the top-wall defects, the simulated image shows at least a qualitative agreement with the observed contrast, the dark and bright pair [Figs. 1(e)–1(h)], in the middle of DWNT. It is hardly possible from these images to distinguish the number of *I*-*V* pairs (one or two in this case) consisting of a "single interlayer bridge." This is mainly

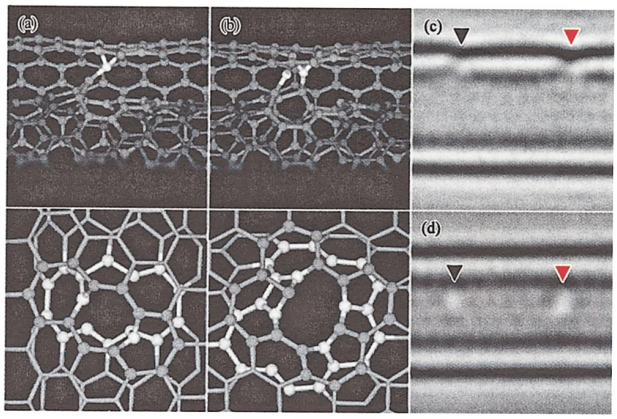

FIG. 2 (color). Expected atomic configurations by using a semiempirical potential and their image simulations of the interlayer defects observed in Fig. 1. (a) A single *I*-*V* pair and (b) a couple of *I*-*V* pairs. (c),(d) Image simulations for the side and top views of the interlayer defects of a single *I*-*V* pair (black arrows) and a couple of *I*-*V* pairs (red arrows).

because of the insufficient spatial resolution of the experiments [15]. It is, however, more than enough to demonstrate the first experimental evidence for the interlayer *I-V* pair defect with a partial sp^3 character to, indeed, arise in between the bilayer of graphite.

Then the temperature dependence of the defect formation in DWNTs is investigated for stability of the defect. Figure 3 shows three sequential HR-TEM images recorded with the same time scale under the same electron dose condition at different temperatures: (a) 93 K, (b) 300 K, and (c) 573 K [16]. A tremendous difference has been found among them. At 93 K, the defects are quite prolific, the inner layer in DWNT is heavily damaged within 140 s, and no tubular structure remains. The interlayer defects are also found frequently at 300 K; some of the defects remain for a certain time, but the others disappear during the observation and the DWNT remains relatively stable. Most interestingly, the interlayer defects can barely be found at 573 K and the DWNT is perfectly resistive to the same amount of electron dose at this temperature. This is attributed to an unstable *I-V* pair at this temperature, and it is quite reasonable for a knocked-on atom to recombine with a vacancy nearby when they come closer. The recombination barrier seems therefore no more effective, and the *I-V* pair defect cannot survive above this temperature [17].

Clustering of vacancies and/or interstitial atoms is more frequently observed at a lower temperature (93 K). This should be due to a possible higher knock-on rate of adjacent carbon atoms nearby the defect created in the previous knock-on event, which could hardly recover. Even for high-temperature observations, the interstitial atoms do not show any activity to move out (as well as the created vacancies that seem totally immobile) and the mobility of the interstitial atoms appears substantially limited in comparison with that for the surface atoms [5]. The recombination barrier of the *I-V* pair defect estimated by the *ab initio* study (1.4 eV) is substantially larger than the surface atom migration barrier (0.6–1 eV) [18] and is smaller than that for vacancy migration (1.7 eV) [19].

To more precisely estimate the critical temperature for the defect annihilation, a systematic HR-TEM observation has been performed at elevated temperatures and the formation rate of the interlayer defects has been plotted in Fig. 4. We just counted the number of defects that show a sufficient contrast in HR-TEM images; therefore we probably underestimated the number of defects because a single *I-V* pair may not give enough contrast to be convincingly isolated from the noise level and may have been missed. To count the number of visible defects should have, however, enough implications to perceive a tendency of the formation rate versus temperature. The number thus counted for clusters of *I-V* pairs found in a DWNT is averaged for several batches at every 50 K and then normalized by the unit area. As seen in Fig. 4, the defect formation rate shows a monotonous decrease versus temperature, and a threshold appears about 450–500 K. Surprisingly, this threshold, indeed, corresponds to the temperature for the Wigner-energy release of about 473 K indicated by a broken line [7].

This work demonstrates that the interlayer defects are quite prolific in an electron-irradiated graphite (the DWNT

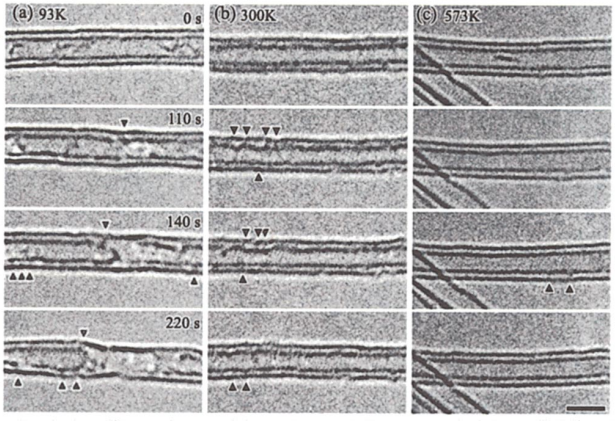

FIG. 3 (color). Sequential HR-TEM images for the formation rates of the interlayer defects at different temperatures with the same time scale (0 to 220 s). (a) At 93 K, the defects due to electron irradiation are quite prolific, and the nanotube inside quickly damages due to the complex defects. (b) At 300 K, the nanotubes are more resistive but the defects can also be found frequently. (c) At 573 K, the defect formation can hardly be seen and the DWNTs are completely resistive due to the electron beam irradiation. The arrows indicate possible interlayer defects. Scale bar = 2 nm.

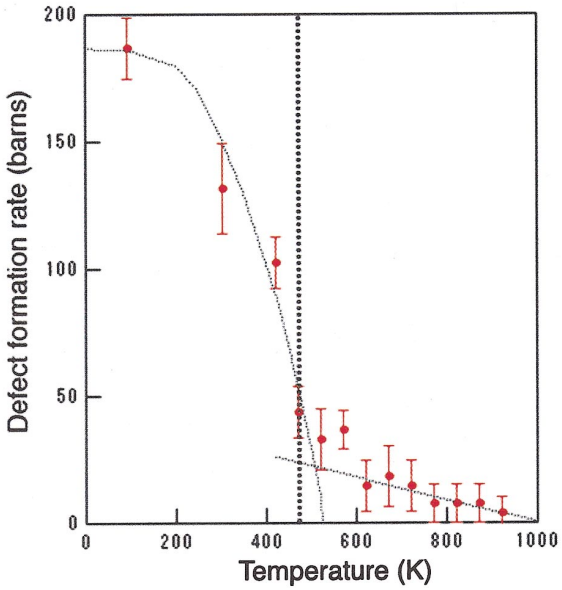

FIG. 4 (color). Normalized formation rate of the clusters of the *I-V* pair defects per unit area of a bilayer estimated in HR-TEM images recorded at different temperatures. The broken line indicates the known temperature for the Wigner-energy release (~ 473 K) (Ref. [7]).

in this case). Since the momentum transfer process in irradiated graphite should be essentially similar for any high-energy particle (such as electron, ion, or neutron), the results can be therefore applicable to interpret the major defect structures in any graphite material used for a high-energy nuclear plant. The temperature for deactivating the recombination barrier found here (450–500 K) is quite close to the annealing temperature for releasing the Wigner energy at 473 K [7]. This can be the first experimental proof for the major defect structure of the graphite in a practical use, which has been clarified at atomic level, and may corroborate the origin of the defect (D) peak in Raman studies of graphite irradiation [20]. Moreover, these interlayer defects demonstrated here must have a strong influence on the transport properties of DWNTs [21,22]. As the interlayer conductivity has been recently pointed out by Bourlon *et al.* [23], the *in situ* transport measurement of a defective DWNT would be of great interest. The constituent nanotubes of DWNT devices may not be independently conducting. Although the defect energetics on the curved graphene layer has not been well discussed in the present study, similar experiments using nanotubes with different diameters as well as small flat graphite with the reduced number of layers would be of great interest to clarify the curvature dependence. In order to verify the beam energy dependence of the defect creation rate, one must change the irradiation energy while keeping the observation energy (at 120 kV, for example). A decreased accelerating voltage should lead to the lower defect creation rate. It is, however, difficult to assign the defect structure with the low beam energy due to the inevitable degraded TEM point resolution.

The work in electron microscopy was supported by the NEDO Nano-carbon Technology project. We thank Professor Morita for his careful reading of the manuscript and fruitful comments.

*To whom correspondence should be addressed.
Electronic address: suenaga-kazu@aist.go.jp

[1] F. Banhart, Rep. Prog. Phys. **62**, 1181 (1999).
[2] B. T. Kelly, *Physics of Graphite* (Applied Science Publishers, London, 1981).
[3] R. H. Telling, C. P. Ewels, A. A. El-Barbary, and M. I. Heggie, Nat. Mater. **2**, 333 (2003).
[4] C. P. Ewels, R. H. Telling, A. A. El-Barbary, and M. I. Heggie, Phys. Rev. Lett. **91**, 025505 (2003).
[5] A. Hashimoto, K. Suenaga, A. Gloter, K. Urita, and S. Iijima, Nature (London) **430**, 870 (2004).
[6] E. P. Wigner, J. Appl. Phys. **17**, 857 (1946).
[7] E. W. J. Mitchell and M. R. Taylor, Nature (London) **208**, 638 (1965).
[8] A. Hashimoto, K. Suenaga, K. Urita, T. Shimada, T. Sugai, S. Bandow, H. Shinohara, and S. Iijima, Phys. Rev. Lett. **94**, 045504 (2005).
[9] T. Iwata and T. Nihira, J. Phys. Soc. Jpn. **31**, 1761 (1971).
[10] M. Takeuchi, S. Muto, T. Tanabe, S. Arai, and T. Kuroyanagi, Philos. Mag. A **76**, 691 (1997).
[11] T. Sugai, H. Yoshida, T. Shimada, T. Okazaki, S. Bandow, and H. Shinohara, Nano Lett. **3**, 769 (2003).
[12] See EPAPS Document No. E-PRLTAO-94-040517 for a series of HR-TEM images (one side view, two top view) in which the interlayer defects are imaged during formation and annihilation. A direct link to this document may be found in the online article's HTML reference section. The document may also be reached via the EPAPS homepage (http://www.aip.org/pubservs/epaps.html) or ftp.aip.org in the directory /epaps/. See the EPAPS homepage for more information.
[13] B. W. Smith and D. E. Luzzi, J. Appl. Phys. **90**, 3509 (2001).
[14] T. Iwata, J. Nucl. Mater. **133–134**, 361 (1985).
[15] The point resolution of the electron microscope used in this experiment (at 120 keV) is about 0.23 nm, and the information limit is about 0.18 nm. They are essentially insufficient to distinguish the detailed atomic structure of a point defect and to justify any relaxed atomic model for the defect (see Ref. [3] for more detailed discussion).
[16] The time scale shown here is the real time. The total dose is typically half of the real time due to the beam blanking used for CCD readout and data acquisition (about 1 s for each image).
[17] There has been a HR-TEM study reported by Yaguchi *et al.* in which more ''clean'' carbon nanotubes were observed at 873 K, but the authors of this paper did not provide any physical explanation about their observation [T. Yaguchi, T. Sato, T. Kamino, Y. Taniguchi, K. Motomiya, K. Tohji, and A. Kasuya, J. Electron Microsc. **50**, 321 (2001)].
[18] A. V. Krasheninnikov, K. Nordlund, P. O. Lehtinen, A. S. Foster, A. Ayuela, and R. M. Nieminen, Phys. Rev. B **69**, 073402 (2004).
[19] A. A. El-Barbary, R. H. Telling, C. P. Ewels, M. I. Heggis, and P. R. Briddon, Phys. Rev. B **68**, 144107 (2003).
[20] E. Asari, M. Kitajima, and K. G. Nakamura, Phys. Rev. B **47**, 11 143 (1993), and references therein.
[21] M. Kociak, K. Suenaga, K. Hirahara, T. Nakahira, Y. Saito, and S. Iijima, Phys. Rev. Lett. **89**, 155501 (2002).
[22] T. Shimada, T. Sugai, Y. Ohno, S. Kishimoto, T. Mizutani, H. Yoshida, T. Okazaki, and H. Shinohara, Appl. Phys. Lett. **84**, 2412 (2004).
[23] B. Bourlon, C. Miko, L. Forró, D. C. Glattli, and A. Bachtold, Phys. Rev. Lett. **93**, 176806 (2004).